1 Executive Summary

- In the regime where $e_{\rm lim}$ is sufficient to induce one-shot mergers, the inclinations I_0 where $e_{\rm lim}$ is attainable correspond very well with the regions where the octupole-induced merger probability is nonzero.
- Furthermore, there are regions where "octupole-enhanced" mergers occur. This is because octupole effects excite the suitably-averaged eccentricity enough that mergers occur within a Hubble time. This effect is much more substantial for smaller a, where one-shot mergers are difficult.
- For I_0 sufficiently close to 90°, finite η suppresses octupole-LK excitation to $e_{\rm lim}$.

2 Simulations

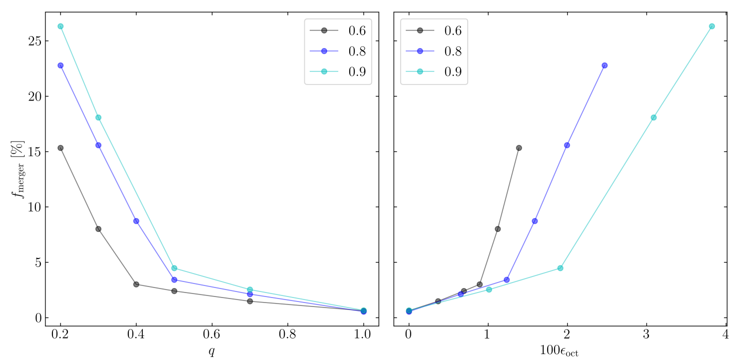

Figure 1: Total merger fractions as a function of q (left) and $\epsilon_{\rm oct}$ (right). Different symbols denote different $e_{\rm out}$ (legend), and different colors denote different $q \in [0.2, 0.3, 0.4, 0.5, 0.7, 1.0]$ (darker colors correspond to smaller q). Only $q = 0.4, e_{\rm out} = 0.9$ is missing.

10 AU is hard to run, RAM intensive and takes many cycles to merger. I tried to run too dense of a grid of simulations and also had some RAM issues on accident, didn't finish. But most of the behavior can be seen in the 100 AU simulations that I ran, which are much faster ($t_{\rm LK} \propto a^{3/2}$).

Tried to run wide range of simulations for $\{q \in [0.2, 0.3, 0.4, 0.5, 0.7, 1.0]\} \otimes \{e_{\rm out} \in [0.6, 0.8, 0.9]\}$ while holding $a_{\rm out,eff} = 3600$ AU ($e_{\rm out} = 0.6$, $a_{\rm out} = 4500$ AU) constant. The other parameters are, as before:

$$m_{12} = 50M_\odot, \qquad m_3 = 30M_\odot, \qquad a_{1,0} = 100\,\text{AU} \qquad e_{1,0} = 10^{-3}.$$

Of the 18 parameter regimes targeted, 17 have complete data. The current merger fraction plot is in Fig. 1.

However, I do reproduce the "gap" that Bin saw. A characteristic plots are shown in Figs. 2–5.

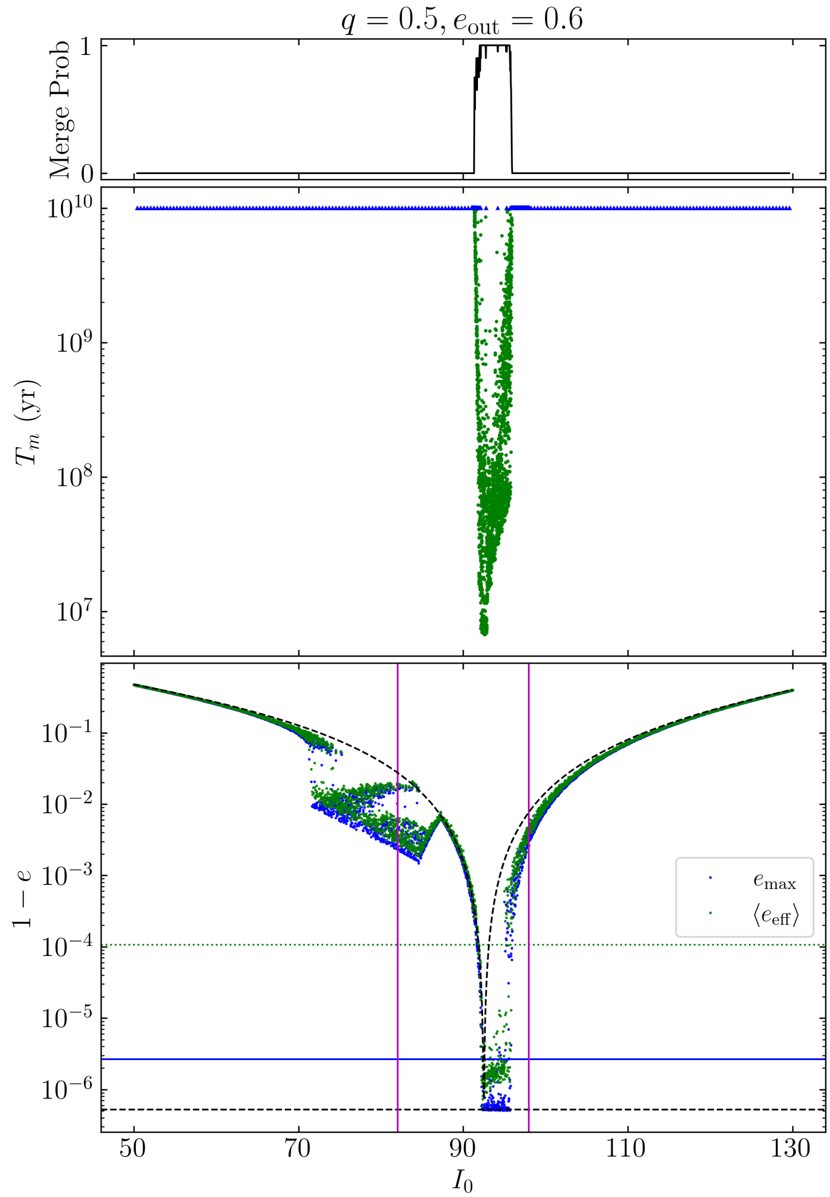

Figure 2: Example 1. Top panel is merger probability, middle panel is merger times (green dots are mergers, blue triangles are non-merging systems), and the bottom panel is the plot of $1-e$ without GW run over $500t_{\rm LK}$. On the bottom panel, the black dashed curve represents the quadrupole $e_{\rm max}$ values [analytic, LL18 Eq. (42)], the blue dots represent the $e_{\rm max}$ over the GW-less run, and the green dots represent the average $e_{\rm eff}$ [Eq. (9)] over the same interval; the horizontal lines correspond to $e_{\rm lim}$ (black), the one-shot merger eccentricity $e_{\rm os}$ (blue), the necessary effective eccentricity to merge $e_{\rm eff,c}$ (green); and the pink vertical lines represent $I_{\rm lim}$ given by MLL16 for reference. In broad summary, systems with $e_{\rm max}$ below the blue line are expected to merge, as are systems with $\langle e_{\rm eff} \rangle$ below the green line.

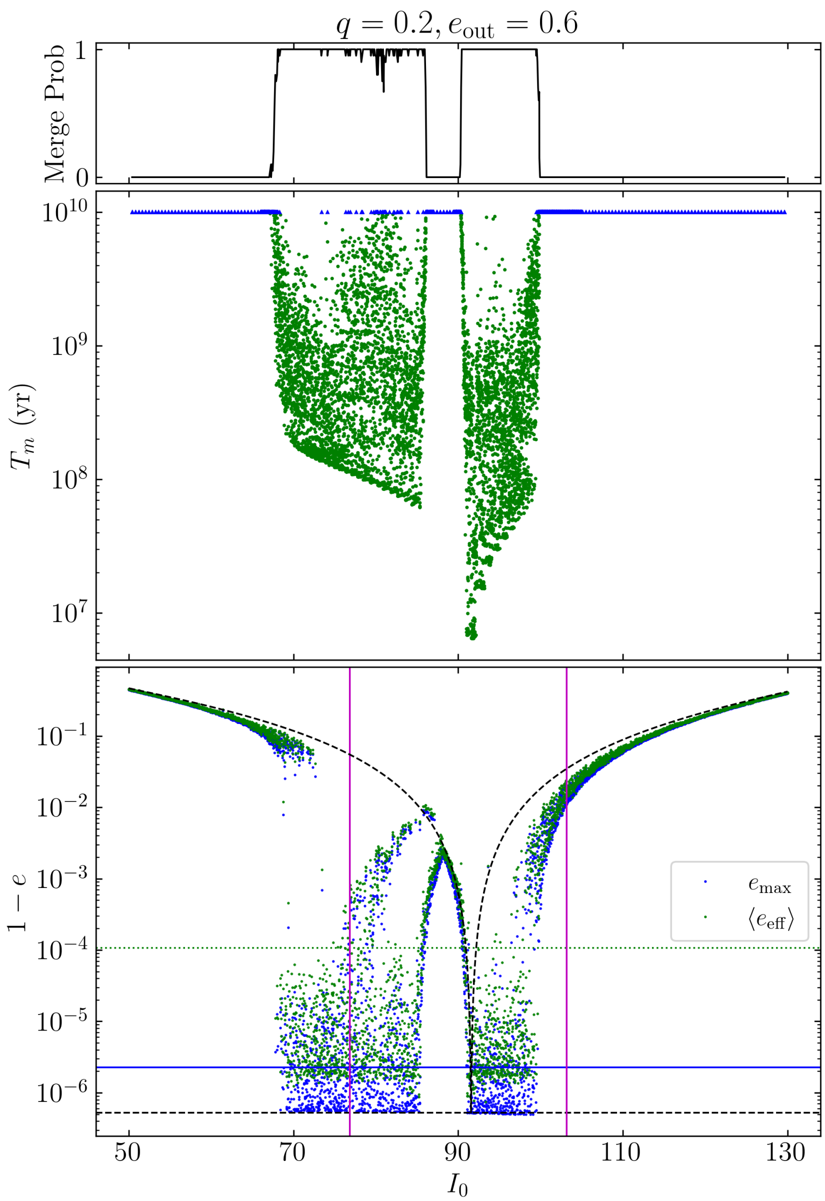

Figure 3: Example 2

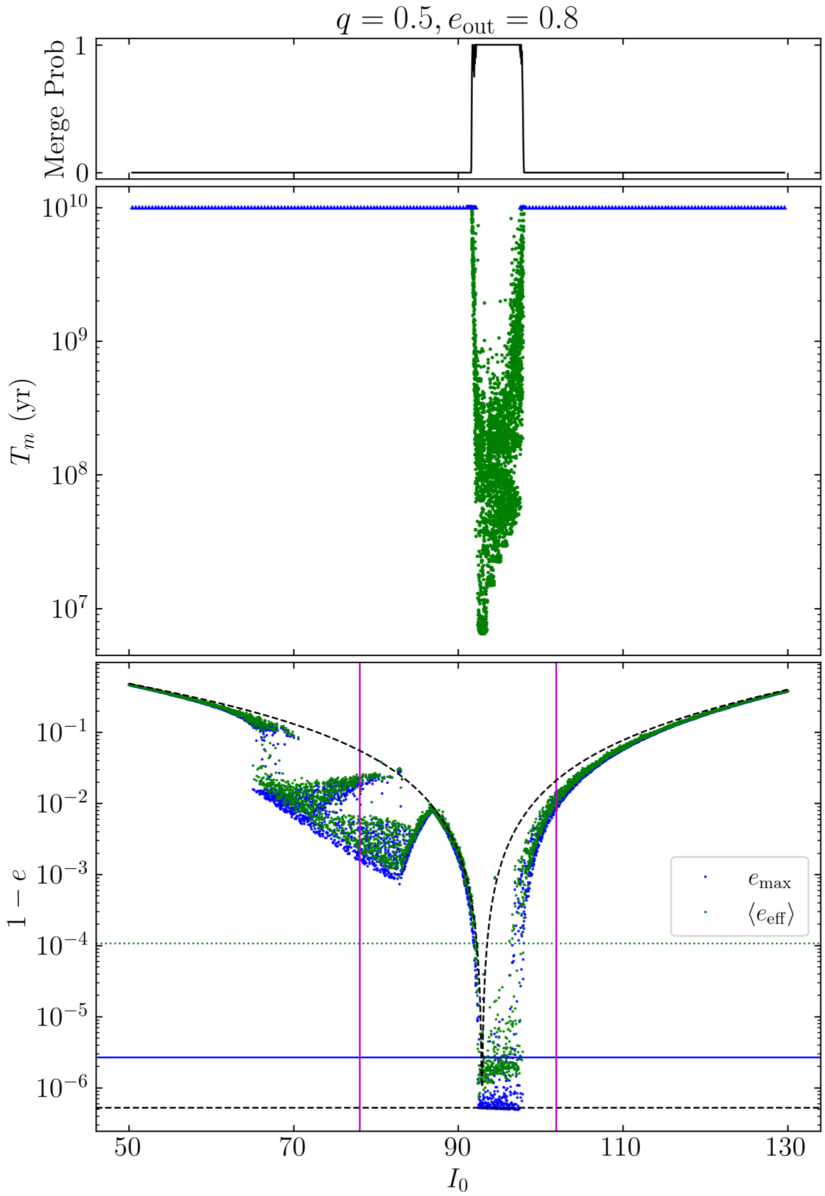

Figure 4: Example 3

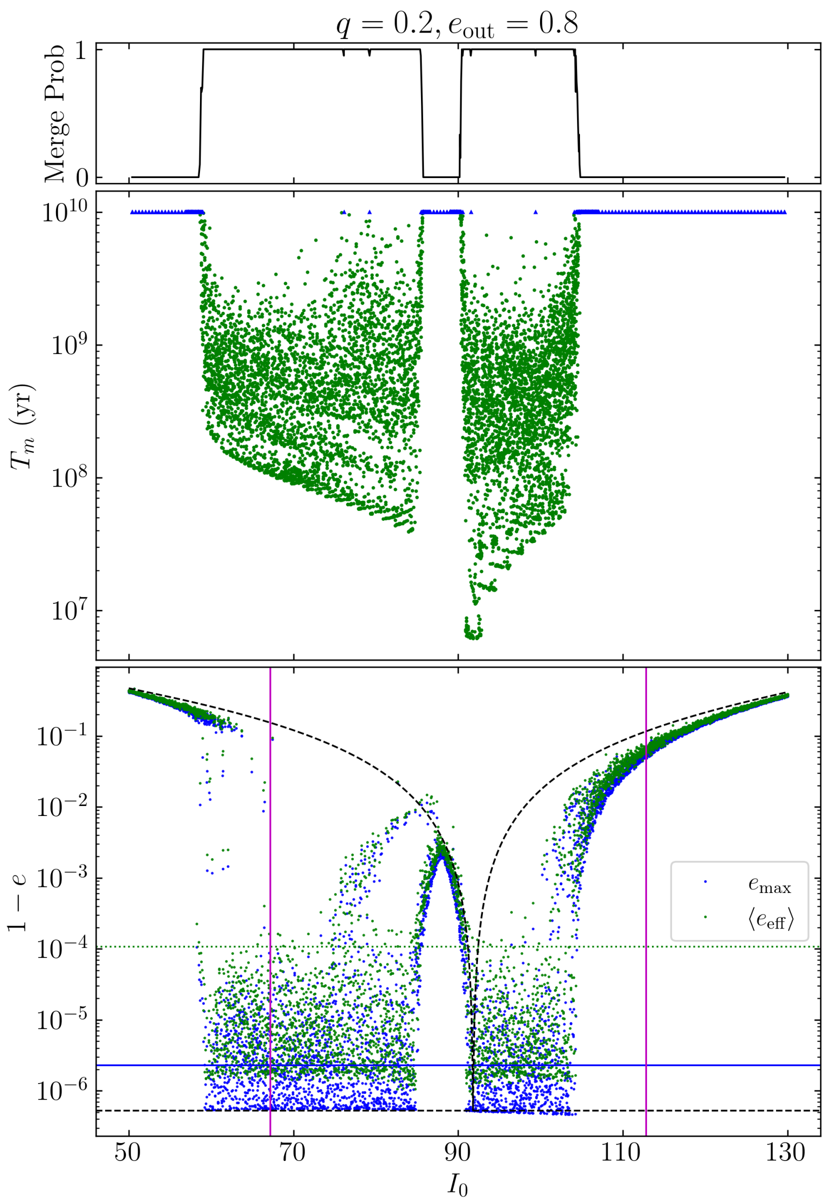

Figure 5: Example 4

3 Theory

3.1 One-Shot Merger Eccentricity

We seek a critical $e_{\rm os}$ for which the system can merge in "one-shot", i.e. in one LK cycle. This can be computed:

$$\frac{\mathrm{d}\ln a}{\mathrm{d}t} = -\frac{64}{5j^7(e)}\left(1+\frac{73}{24}e^2+\frac{37}{96}e^4\right)\frac{G^3\mu m_{12}^2}{c^5a^4}, \tag{1}$$

$$\left\langle\frac{\mathrm{d}\ln a}{\mathrm{d}t}\right\rangle_{\rm LK} \sim -j(e_{\max})\frac{64}{5j^7(e_{\max})}(4)\frac{G^3\mu m_{12}^2}{c^5a^4} = \frac{1}{t_{\rm GW,0}j^6(e_{\max})}, \tag{2}$$

$$j^6(e_{\rm os}) \equiv j_{\rm os} = \frac{t_{\rm LK}}{t_{\rm GW,0}}, \tag{3}$$

$$= \frac{256}{5}\frac{G^3\mu m_{12}^3}{m_3c^5a^4n}\left(\frac{a_{\rm out,eff}}{a}\right)^3, \tag{4}$$

where $t_{\rm GW,0}$ denotes the $e=0$ evaluation of the GW inspiral timescale, and angle brackets denote averaging over a *single* LK cycle. Thus, when systems satisfy $e_{\rm lim} \gtrsim e_{\rm os}$, all orbit flips will immediately lead to mergers. We can estimate

$$j_{\rm lim} \approx \frac{8\epsilon_{\rm GR}}{9+3\eta^2/4}, \tag{5}$$

$$\left(\frac{a}{a_{\rm out,eff}}\right) \gtrsim 0.0118\left(\frac{a_{\rm out,eff}}{3600\,\mathrm{AU}}\right)^{-7/37}\left(\frac{m_{12}}{50M_\odot}\right)^{17/37}\left(\frac{30M_\odot}{m_3}\right)^{10/37}\left(\frac{q/(1+q)^2}{1/4}\right)^{-2/37}. \tag{6}$$

This is the regime in which ELK-induced mergers is easiest to understand.

3.2 Effective Merging Eccentricity

Some systems can merge even without undergoing orbit flips. These correspond to the probabilistic regions. We define an "effective" eccentricity, over the GW-less simulations, such that the total GW emission is comparable:

$$\left\langle\frac{\mathrm{d}\ln a}{\mathrm{d}t}\right\rangle_{\rm LK} = -\left\langle\frac{a}{t_{\rm GW}}\right\rangle_{\rm LK}, \tag{7}$$

$$\approx -\frac{a}{t_{\rm GW,0}}\left\langle\frac{1+73e_{\max}^2/24+37e_{\max}^4/96}{j^6(e_{\max})}\right\rangle, \tag{8}$$

$$\left\langle\frac{\mathrm{d}\ln a}{\mathrm{d}t}\right\rangle_{\text{Many LK Cycles}} \equiv -\frac{a}{t_{\rm GW,0}}\underbrace{\left(\frac{1+73e_{\rm eff}^2/24+37e_{\rm eff}^4/96}{j^6(e_{\rm eff})}\right)}_{f(e_{\rm eff})} \approx \frac{-4a}{t_{\rm GW,0}j^6(e_{\rm eff})} \tag{9}$$

where the second average is taken over many LK cycles, as denoted.

Comment after meeting: Note that formulating $e_{\rm eff}$ by averaging over just eccentricity *maxima*, rather than the full $e(t)$, may have advantages if we are able to estimate the octupole-induced oscillation amplitude of K [Eq. (13), see discussion at the end of Section 3.3].

We can then ask what level of $e_{\rm eff}$ is required to induce merger within a Hubble time $t_{\rm Hubb}$. This

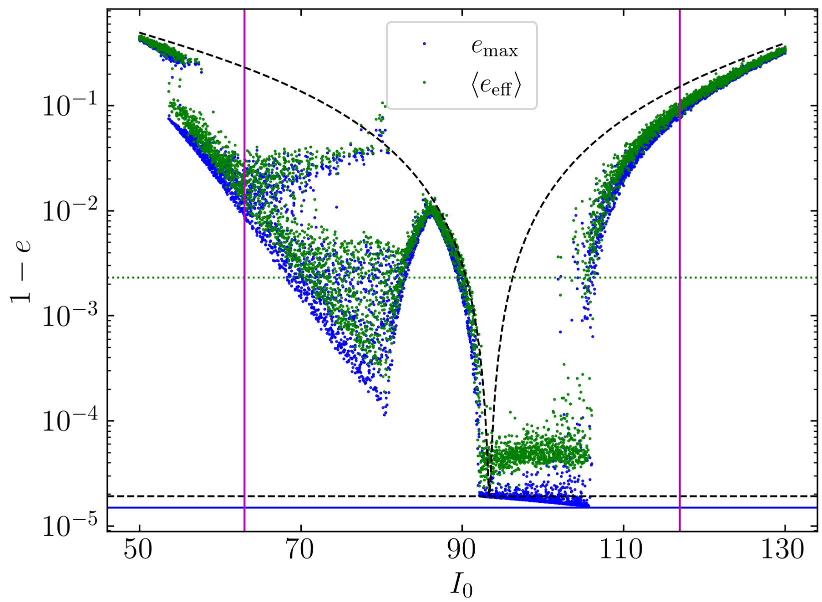

Figure 6: $e_{\max}$ distribution for Bin's gapped case last week. Note that $e_{\rm lim} \approx e_{\rm os}$ for this parameter regime.

can also be estimated

$$\frac{t_{\rm GW,0}}{t_{\rm Hubb}} \frac{1}{f(e_{\rm eff})} \lesssim 1, \tag{10}$$

$$\left(\frac{4t_{\rm Hubb}}{t_{\rm GW,0}}\right)^{1/6} \gtrsim j(e_{\rm eff}), \tag{11}$$

$$0.01461 \left(\frac{100\,\mathrm{AU}}{a}\right)^{2/3} \left(\frac{1/4}{q(1+q)^2}\right)^{1/6} \gtrsim j(e_{\rm eff}). \tag{12}$$

We can see that the probabilistic regime in the earlier figures is where $e_{\rm eff}$ spans a few orders of magnitude. This suggests that $e_{\rm eff}$ stochastically attains these large values over timescales $\gg 500 t_{\rm LK}$ (i.e. over time, some fraction of systems will enter a very high maximum-eccentricity state).

3.3 Origin of the Gap

We have already reproduced the gap in our simulations. For reference, we can also look at $e_{\max}$ distribution for Bin's case from last week $a_{\rm out} = 700$, $e_{\rm out} = 0.9$, $a_{\rm in} = 10\,\mathrm{AU}$, and $q = 0.4$ in Fig. 6 (NB: I messed up and used $m_{12} = 50 M_\odot$ while Bin used $m_{12} = 60 M_\odot$).

The origin of the gap is because $e_{\max}$ oscillations are suppressed near $I = 90^\circ$. I think this happens because Katz et. al. 2011 show that ELK oscillations happen due to a feedback between $j_z = j\cos I$ (conserved to quadrupole order in the test mass limit) and Ω_e the co-longitude (azimuthal angle relative to $\hat{\mathbf{z}}$) of the inner eccentricity vector. However, when $\eta > 0$, we know that the conserved quantity is (LL18)

$$K \equiv j\cos I - \eta \frac{e^2}{2}. \tag{13}$$

This suggests that when $|j\cos I| \lesssim \eta/2$, that η suppresses oscillations in $j\cos I$ and the oscillations in the eccentricity maxima. I think this is the right mechanism, but I don't have the analytical solution.

I add two plots I showed last week, to illustrate the oscillations in K and their effect on the behavior of $e_{\max}$, shown in Fig. 7. We see that K oscillates (albeit somewhat irregularly) over timescales much longer than a LK cycle. This may allow us to estimate the $e_{\rm eff}$ enhancement expected due to octupole effects when orbital flips are not observed.

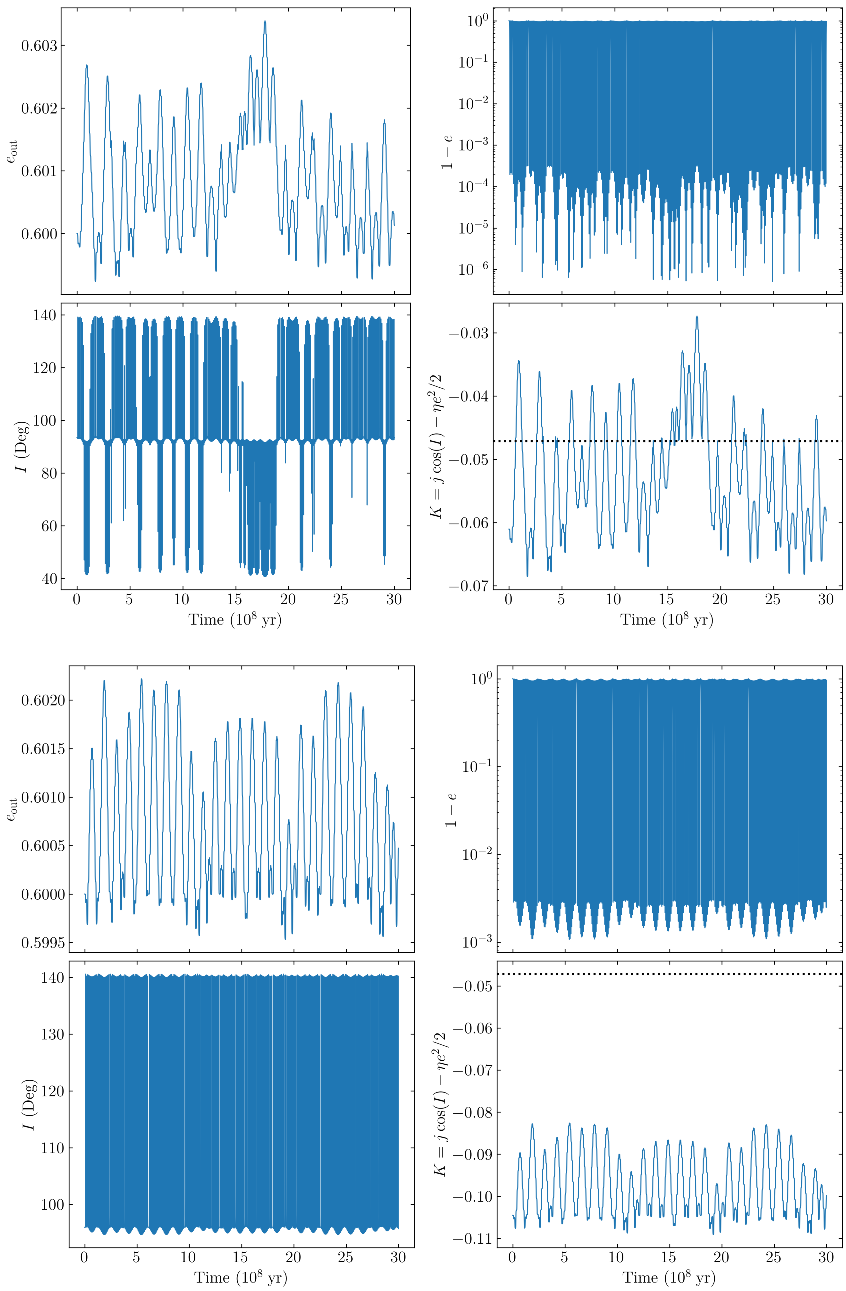

Figure 7: Two fiducial simulations showing the behavior of K in the absence of GW radiation. Here, $q = 2/3$. In the fourth panels of both simulations, the horizontal black dotted line gives $K = -\eta_0/2$, where orbital flips are expected.